*Journal of Sound and Vibration* (2000) **238**(4), 710–719
doi:10.1006/jsvi.2000.3017, available online at http://www.idealibrary.com on IDEAL®

# PREDICTION OF TORSIONAL DAMPING COEFFICIENTS IN RECIPROCATING ENGINE

Y. Wang and T. C. Lim

*Department of Mechanical Engineering*, 290 *Hardaway Hall*, *Box* 870276, *The University of Alabama*, *Tuscaloosa*, *AL* 35487, *U.S.A.*

(*Received* 25 *February* 2000)

## 1. INTRODUCTION

It is generally known that the torsional vibration characteristics of rotating components in reciprocating internal combustion (IC) engines are critical to powertrain noise and durability concerns. Excessive vibratory response can lead to significant boom noise response, and in extreme conditions can cause premature structural failure. Therefore, in an effort to improve engine design and prevent undesirable noise and vibration problems, researchers have devoted much attention to the development of suitable dynamic models to gain further insight into the vibratory behavior and identify important design parameters [1–5]. In many cases, the validity and usefulness of the models depend on the knowledge of the precise mass moment of inertia, stiffness and damping values. Of these three sets of parameters, damping is typically the most difficult one to determine accurately.

Studies of global damping effect in reciprocating engines can be traced back to the early 1930s [6]. Later, researchers such as Den Hartog, Draminsky, Ker Wilson and others [1, 7–9] started to focus more attention on the specific origins of damping in the different engine parts. Most of the damping parameters applied was empirically determined from experimental observations made on specific reciprocating engine systems. Their values are frequently inaccurate, resulting in significant variation in the simulated vibration response [10]. In addition, theoretical and hybrid damping models have also been proposed such as in reference [11], which led to analytical relationships between damping and other more tangible engine parameters. In spite of recent progress, the accuracy of the damping representation in reciprocating engines and the knowledge of how it varies with crank angle are still unsatisfactory. Also, the significance of the individual damping present is poorly understood. Hence, to aid in achieving a better understanding of the damping characteristics, the problem of analyzing the torsional damping coefficients in reciprocating IC engines by applying the equivalent vibratory energy approach is considered here.

Among the many existing vibration models of rotating engine components, the lumped parameter representation is one of the simplest and most commonly applied theories. In spite of the sacrifice in modelling elegance, the lumped parameter approach can still achieve sufficient accuracy for many practical applications given a suitable set of parameters [12]. It is applied here as the basis for the present damping identification analysis. Also, only the angular degree of freedom (d.o.f.) of the rotating components is considered, as our analysis primarily concentrates on the prediction of the torsional damping coefficients. Using an experimental set-up comprising of a single-cylinder reciprocating engine, the instantaneous

0022-460X/00/490710 + 10 $35.00/0 

damping coefficients corresponding to the first two flexible torsional modes are obtained for different crank angle positions. This is accomplished by assuming a series of discrete quasi-static configurations. The same test set-up is also applied under steady state motoring condition to determine the time-averaged damping coefficients for comparison with the time-varying results.

## 2. FORMULATION

Consider a vertical single-cylinder reciprocating engine system whose crank is attached by means of a shaft–flywheel element to an electric DC motor, as illustrated in Figure 1. The single-cylinder unit with a cross-head is designed with a relatively long stroke to enhance the effect of hysteretic damping in the piston–cylinder head interface. If only the angular perturbation response of the structure about its rotational axis is considered, then by using the classical lumped parameter approach, a discrete $n$-dimensional model, where $n = 8$ for the complete system described in Figure 1, can be defined explicitly as shown in Figure 2.

The lumped mass moment of inertia $I_i$ associated with each torsional co-ordinate $\varphi_i$ of the model is determined by applying either the circular/annular disk equation for axisymmetric rotating geometries like the shaft, flywheel and motor, or the equivalent kinetic energy expression for more complex structures like the piston, connecting rod and crank. The former calculation is quite trivial and will not be dealt with in detail here. In the latter case, given the combined mass of the piston and cross-head to be $m_s$, and the top and bottom parts of connecting rod as $m_A$ and $m_B$, respectively, it can be shown that the kinetic energy-equivalent lumped mass moment of inertia of the combined single-cylinder bodies in motion as a function of crank angle $\alpha$ is given as

$$I_3(\alpha) = R^2(m_S + m_A)(\sin(\alpha) + \cos(\alpha)\tan(\beta))^2 + m_B R^2 + I_R, \tag{1}$$

where $R$ is the crank radial distance, $I_R$ is the crank mass moment of inertia about the rotational axis, and $\beta$ is the acute angle bounded by the centerline of the connecting rod and vertical axis. The above equation is derived by collapsing the kinetic energies of the individual reciprocating masses into a single energy term. Due to the dependency of equation (1) on $\alpha = \int \Omega \, dt$ where $\Omega$ is the mean angular velocity and $t$ is the time scale, the calculation produces a time-dependent diagonal inertia-matrix term $[I(t)]$. The corresponding stiffness coefficient matrix $[K]$ of the shaft elements is derived from the torsional rigidity equation of a uniform bar, which is inherently time-invariant. Note that in

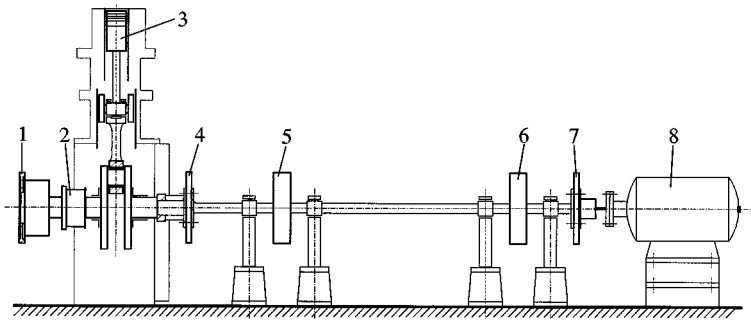


Figure 1. Vertical single-cylinder engine set-up: 1, measurement gear; 2, attachment disk; 3, cylinder; 4, measurement gear; 5, flywheel; 6, flywheel; 7, universal joint/measurement gear; 8, DC motor.

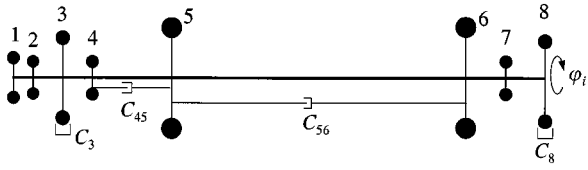


Figure 2. Lumped parameter model of the proposed single-cylinder engine system.

this approach, the crank and connecting rod are assumed to be infinitely rigid, and thus allowing us to neglect their time-varying compliance effect. The equation of torsional vibration motion in matrix form is

$$[I(t)]\{\ddot{\varphi}(t)\} + [C(t)]\{\dot{\varphi}(t)\} + [K]\{\varphi(t)\} = \{T(t)\}, \tag{2}$$

where $\{\varphi(t)\}$ is the angular displacement vector, $\{T(t)\}$ is the externally applied periodic torque fluctuation vector, and $[C(t)]$ is the time-varying equivalent viscous damping coefficient matrix. The non-zero damping terms used to form $[C(t)]$ are depicted in Figure 2. They include the absolute damping coefficients $c_i$ of the cylinder ($i = 3$) and motor ($i = 8$), and the relative damping coefficients $c_{i,i+1}$ of the two damped drive shaft segments ($i = 4, 5$). The two absolute damping terms $c_i$ are the primary emphasis of this communication, which are to be obtained experimentally. On the other hand, the relative damping coefficients are computed using an empirical equation given by $c_{i,i+1} = 0{\cdot}04259/\pi\omega e_{i,i+1}$, where $\omega$ is the frequency in rad/s and $e_{i,i+1}$ is the flexibility of the shaft segment between points $i$ and $i + 1$, which was developed from experimental evidences as reported in reference [12].

Letting $\{T(t)\} = \{0\}$ and considering only the inertia and stiffness matrices in equation (2) leads to the classical free-vibration problem. Assuming harmonic motion $\{\varphi(t)\} = \{\vartheta\}e^{j\omega t}$ where $j = \sqrt{-1}$, we obtain the eigenvalue problem given by $[[K] - [I(t)]\omega^2]\{\vartheta\} = 0$. For a specific crank angle position, the inertia matrix can be taken to be time-invariant. This leads to the characteristic equation expressed as $\det([K] - [I(\alpha)]\omega^2) = 0$ where the operator det( ) is the determinant of the undamped dynamic stiffness matrix of equation (2). The solution essentially provides a set of eight unique eigenvalues or natural frequencies $\omega_p = 0, \omega_1, \omega_2, \ldots, \omega_{n-1}$, where the first one represents the rigid body motion at zero frequency, while the others are flexible torsional modes. In this analysis, we focus mainly on the first two non-zero natural modes at $\omega_1$ and $\omega_2$. By varying $\alpha$, we can compute the time-varying natural modes quasi-statically. The same free-vibration calculation can also be performed using the average mass moment of inertia $\tilde{I}_3$ for the cylinder bodies to produce a constant set of average natural frequency $\tilde{\omega}_p$. Note that $\tilde{I}_3$ can be computed by integrating $I_3(\alpha)$ over a complete crank angle cycle and normalizing the result by $2\pi$ rad. For the system described in Figure 1 whose time-invariant parameters and natural modes are given in Table 1, Figures 3(a, b) show the predicted dimensionless inertia $I_3(\alpha)/\tilde{I}_3$ and the natural frequency $\omega_p/\tilde{\omega}_p$ terms of $p = 1$ and 2, respectively, as a function of $\alpha$ ranging from 0 to 180°. The results are not shown up to 360° since the other half of $\alpha$ is symmetrically identical. As one can see from the plot, the variation in the first two natural frequencies is less than 10 per cent. Its magnitude is also inversely proportional to the normalized inertia as expected. The corresponding average mode shapes are illustrated in Figure 4. Due to the dependency of the effective inertia on $\alpha$, the actual modes are not invariant but depict slight spatial variation as the crank is displaced through a complete cycle. However, the fundamental nature of the first two mode shapes that is of primary concern here is essentially unchanged.

TABLE 1

*Average parameters and natural modes of the single-cylinder system*

| *Node i* | $I_i$ (kg m$^2$) | $e_{i,i+1}$ (rad/Nm) | Mode-1 $\{\Delta_i\}_1$ | Mode-2 $\{\Delta_i\}_2$ | $c_{i,i+1}$ (Nms/rad) Mode-1 | $c_{i,i+1}$ (Nms/rad) Mode-2 | $c_i$ (Nms/rad) |
|---|---|---|---|---|---|---|---|
| 1 | 0·021228 | $1{\cdot}2405 \times 10^{-6}$ | 1·00000 | 1·00000 | 0 | 0 | 0 |
| 2 | 0·004889 | $3{\cdot}0863 \times 10^{-6}$ | 0·99906 | 0·99326 | 0 | 0 | 0 |
| 3 | 0·083485 | $5{\cdot}8404 \times 10^{-6}$ | 0·99611 | 0·97206 | 0 | 0 | $c_3(\alpha)$ |
| 4 | 0·011603 | $5{\cdot}2920 \times 10^{-5}$ | 0·97275 | 0·80708 | 1·4022 | 0·5111 | 0 |
| 5 | 0·164264 | $1{\cdot}8673 \times 10^{-4}$ | 0·73921 | − 0·81838 | 0·3974 | 0·1485 | 0 |
| 6 | 0·164124 | $5{\cdot}2399 \times 10^{-6}$ | − 0·91487 | 0·05857 | 0 | 0 | 0 |
| 7 | 0·010819 | $8{\cdot}9304 \times 10^{-6}$ | − 0·93248 | 0·06990 | 0 | 0 | 0 |
| 8 | 0·085296 | — | − 0·95921 | 0·08746 | 0 | 0 | $c_8$ |

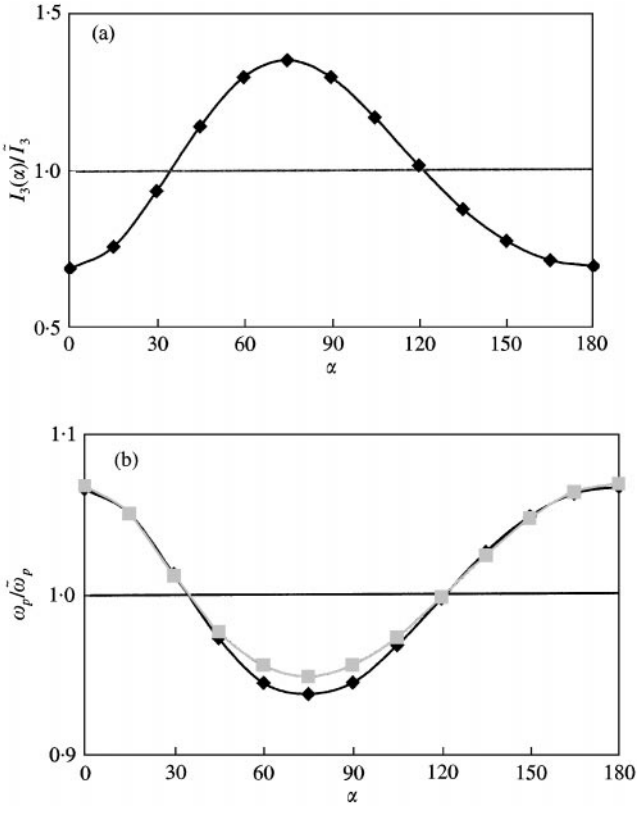


Figure 3. Effect of crank angle $\alpha$ on (a) the normalized inertia $I_3(\alpha)/\tilde{I}_3$, and (b) the first two non-zero natural frequencies $\omega_p/\tilde{\omega}_p$. Here, $\tilde{I}_3 = 0{\cdot}083458$ kg m$^2$, $\tilde{\omega}_1 = 30{\cdot}45$ Hz, and $\tilde{\omega}_2 = 81{\cdot}68$ Hz: ◆, $\omega_1$; □, $\omega_2$.

The preceding free-vibration result is now used to formulate the unknown damping coefficient of the single-cylinder component. First, we note that the overall damping effect may originate from different parts of the single-cylinder unit that include the contact surface areas between the reciprocating piston/cross-head and fixed cylinder; connecting rod and

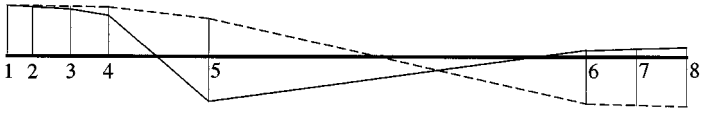


Figure 4. First two flexible mode shapes based on average mass moment of inertia terms: - - - , mode 1; —, mode 2.

cross-head; crank and connecting rod; and main journal bearings and crankshaft. Contribution from the individual damping is the subject of future study. In the current analysis, we are interested in obtaining the net effect of vibratory energy dissipation expressed in terms of the equivalent viscous damping coefficient $c_3(\alpha)$, even though the fundamental nature of the damping also includes the hysteresis phenomenon. The dependence of this single-cylinder damping coefficient on $\alpha$ is expected due to the change in the relative velocity amplitudes at the various contact interface areas given a fixed level of angular fluctuation input at the crank as it takes up different $\alpha$ value. For instance, the total translation displacement of the piston head is the sum of the mean $X$ and perturbed $x$ components:

$$X + x = R[1 - \cos(\alpha + \varphi_3)] + R\lambda[1 - \cos(2\alpha + 2\varphi_3)]/4, \tag{3}$$

where $\lambda$ is the ratio of $R$ to the length of the connecting rod. Assuming small perturbation in which $\sin(\varphi_3) \approx \varphi_3$ and $\cos(\varphi_3) \approx 1$, and taking the time derivative of the above equation gives the mean and perturbed velocities of the piston head as

$$\dot{X} = R\Omega[\sin(\alpha) + \lambda \sin(2\alpha)/2], \quad \dot{x} = R\dot{\varphi}_3[\sin(\alpha) + \lambda \sin(2\alpha)/2], \tag{4a, b}$$

which clearly demonstrates the dependency on $\alpha$. Since the degree of vibratory energy dissipations, especially from hysteresis, is affected by the relative velocity term, we expect the equivalent damping coefficient term to be a function of $\alpha$ as well. The same effect can be seen in the expression for the swing angle of the connecting rod $\beta$ and its corresponding perturbation angle $\gamma$ given by

$$\beta + \gamma = (\lambda + \lambda^3/8)\sin(\alpha + \varphi_3) - \lambda^3 \sin(3\alpha + 3\varphi_3)/24. \tag{5}$$

Similarly for small $\varphi$, the corresponding angular velocity terms can be obtained by taking the time derivative of equation (5),

$$\dot{\beta} = \Omega\,[(\lambda + \lambda^3/8)\cos(\alpha) - \lambda^3 \cos(3\alpha)/8], \quad \dot{\gamma} = \dot{\varphi}[(\lambda + \lambda^3/8)\cos(\alpha) - \lambda^3 \cos(3\alpha)/8], \tag{6a, b}$$

which is obviously a function of $\alpha$ as well. However, notice that the piston perturbation velocity $\dot{x}$ is greatest at $\alpha = \pi/2$ rad, while $\dot{\gamma}$ is largest at $\alpha = 0$ which is exactly 90° apart. The importance of this observation in revealing the more dominant effect will be evident in the experimental analysis later.

Now consider the forced response problem where $\{T(t)\}$ is not completely zero due to an externally applied harmonic torque excitation $T_k(t) = |T_k|e^{j\omega t}$ at a specific point $k$. The vibratory power injected into the system matches the total power dissipated by the damping ($c_i$, and $c_{i,i+1}$) present. Equating the injected and dissipated power terms at resonance, where $\omega = \omega_p$ and the response lags the excitation input by $\pi/2$ rad, leads to the algebraic expression

$$|T_k|\varphi_k = \sum_i^n c_i \omega_p \varphi_i^2 + \sum_i^{n-1} c_{i,i+1}\omega_p(\varphi_i - \varphi_{i+1})^2 \tag{7}$$

for each natural mode of the system. Since the angular displacement response can be expressed as $\varphi_i = \varphi_1 \Delta_i$, where $\{\Delta_i\}_p$ is the eigenvector corresponding to $\omega_p$ in which $\Delta_1$ is normalized to unity, the above equation can be re-written as

$$|T_k|\Delta_k = \omega_p \varphi_1 \left[ \sum_i^n c_i \Delta_i^2 + \sum_i^{n-1} c_{i,i+1}(\Delta_i - \Delta_{i+1})^2 \right], \tag{8}$$

where $\varphi_1$ is the measured angular displacement response of the disk at point 1. This formulation essentially forms the basis for computing the equivalent damping effect of the single-cylinder unit, which can be applied for both quasi-static and running conditions. To apply equation (8), $|T_k|$, $\{\Delta_i\}$ and other non-cylinder related damping terms must be known first. The amplitude of the harmonic torque excitation $|T_k|$ can be either sensed experimentally or computed theoretically, while $\{\Delta_i\}$ is obtained from the eigenvalue analysis of the free-vibration problem. Recall that $c_3$, $c_8$, $c_{4,5}$ and $c_{5,6}$ are the only non-zero damping coefficients as described earlier. However, of these four terms, only $c_3$ and $c_8$ are the unknowns and will be examined experimentally next.

## 3. EXPERIMENTAL RESULTS

An experimental set-up of the single-cylinder engine system shown in Figure 1 is developed for this study. The design specifications of the reciprocating cylinder component used is given by: bore = 72 mm, stroke = 150 mm, $R$ = 75 mm and $\lambda = 0{\cdot}315$. The set-up is used for both quasi-static and running experiments. The former method allows us to determine the cylinder damping coefficients at discrete intervals of crank angle positions, while the latter one produces the average damping term. In both cases, the torsional vibration signals for numerous disk positions are acquired. In the quasi-static experiment, three pairs of linear accelerometers are located at 180° separation, and identical radial distance points from the rotation center are utilized. For the running test, three non-contacting magnetic pickup transducer are used instead. The measured time response is processed using the fast fourier transform technique to compute the response spectra. Note that only the free-end response point is used directly in the calculation, while the other two measured response points are used mainly for a partial validation check of the mode shape vector $\{\Delta_i\}$. The overall set-up is shown in Figure 5.

To determine the damping coefficient of the DC motor first, the cylinder component is physically disconnected from the upstream shaft–flywheel–motor subsystem whose parameters are given in Table 2. By offsetting the angular alignment of the universal joint between the motor and drive shaft such that the driving and driven axes are not collinear, we can produce a periodic torsional excitation about the mean motor speed. The model parameters given in Table 2 are considered time-invariant due to the axisymmetric nature of the remaining subsystem. Accordingly, equation (2) can be reduced to a 5-d.o.f. lumped parameter system with $c_8$ as its only unknown by eliminating the terms associated with the truncated co-ordinates $\varphi_1$, $\varphi_2$ and $\varphi_3$. Solving the corresponding eigenvalue problem gives the first flexible natural mode at $\bar{\omega}_1 = 35$ Hz. The corresponding mode shape in which $\Delta_4$ is normalized to unity is also listed in Table 2. Using $\varphi_i = \varphi_4 \Delta_i$, equation (7) reduces to

$$|T_7|\Delta_7 = \Omega_1 \varphi_4 [c_8 \Delta_8^2 + c_{4,5}(\Delta_4 - \Delta_5)^2 + c_{5,6}(\Delta_5 - \Delta_6)^2], \tag{9}$$

where $T_7 = 4I_7\Omega_1^2[1 - \cos^2(\theta)]/[1 + \cos^2(\theta)]\sin(2\Omega t)$, which can be used to solve $c_8$. Here, $\theta$ is the angular misalignment of the universal joint. Note that in order to obtain an accurate value for $\varphi_4$ at $\bar{\omega}_1$, the running test is performed by sweeping the speed from approximately

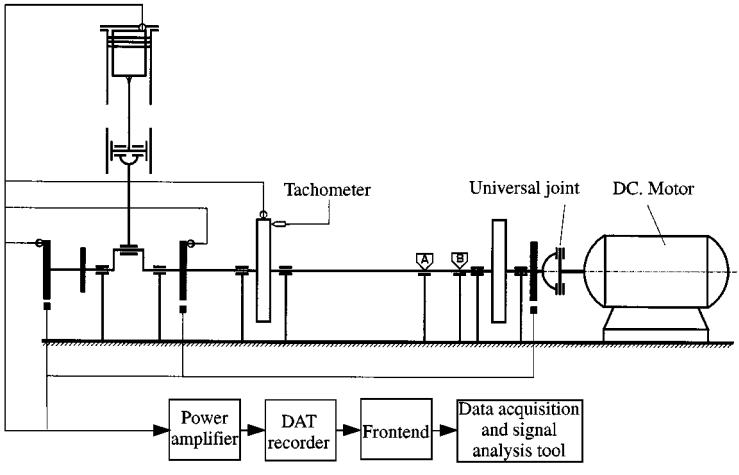


Figure 5. Experimental set-up to perform torsional vibration measurements of quasi-static and running conditions: ◐, accelerometer (quasi-static test); ▮, magnetic pickup transducer (running test); Ⓐ, nodal point for mode 1 (quasi-static test); Ⓑ, nodal point mode 2 (quasi-static test).

TABLE 2

*Average parameters and natural modes of the shaft–flywheel–motor subsystem*

| Node, $i$ | $I_i$ (kg m$^2$) | $e_{i,i+1}$ (rad/Nm) | $\{\Delta_k\}$ | $c_{i,i+1}$ (Nms/rad) | $c_i$ (Nms/rad) |
|---|---|---|---|---|---|
| 4 | 0·009926 | $5{\cdot}2920 \times 10^{-5}$ | 1·00000 | 1·1366 | 0 |
| 5 | 0·164264 | $1{\cdot}8673 \times 10^{-4}$ | 0·97331 | 0·3221 | 0 |
| 6 | 0·164124 | $5{\cdot}2399 \times 10^{-6}$ | − 0·63758 | 0 | 0 |
| 7 | 0·010819 | $8{\cdot}9304 \times 10^{-6}$ | − 0·65493 | 0 | 0 |
| 8 | 0·085296 | | − 0·68128 | | $c_8$ |

850–1300 revolution per minute (r.p.m.), which effectively provides a torque fluctuation frequency that is twice the driving speed, to seek out the specific resonance point. Given the numerical data in Table 2, the motor damping coefficient $c_8$ is found to be 1·6136 Nms/rad.

We are now in the position to set-up the experiment to determine $c_3$. The quasi-static case is considered here. Using the complete installation in which the cylinder is re-attached back to the upstream subsystem, the nodal locations of the first or second total system modes between points 5 and 6 are clamped-down. This is done to set-up artificial boundary conditions that produce natural models (of the downstream subsystem containing the cylinder) that are identical to the total system natural modes. In addition, the fixed point eliminates rigid body motion and eases testing. Table 3 summarizes the parameters for this configuration. Since the motor is isolated from the cylinder–shaft subsystem by the fixed point, an artificial harmonic torque excitation is applied to $\varphi_5$ using a pair of out-of-phase, non-contacting magnetic exciters. The exciter is used to perform frequency sweep between 20–55 and 50–100 Hz to seek out the first two resonances. Equation (8) then simplifies to become

$$|T_5|\Delta_5 = \omega_p \varphi_1 [c_3 \Delta_3^2 + c_{4,5}(\Delta_4 - \Delta_5)^2 + \hat{c}_{5,6}\Delta_5^2], \tag{10}$$

where $\hat{c}_{5,6}$ is the damping coefficient of the shortened shaft as the result of the fixed boundary point. With only one unknown, the above equation can be used to solve $c_3$. This

TABLE 3

*Parameters and natural modes of the clamped single-cylinder system*

| *Node i* | $I_i$ (kg m$^2$) | $e_{i,i+1}$ (rad/Nm) | Mode-1 $\{\Delta_i\}_1$ | Mode-2 $\{\Delta_i\}_2$ | $c_{i,i+1}$ (Nms/rad) Mode-1 | $c_{i,i+1}$ (Nms/rad) Mode-2 | $c_i$ (Nms/rad) |
|---|---|---|---|---|---|---|---|
| 1 | 0·021228 | $1{\cdot}2045 \times 10^{-6}$ | 1·00000 | 1·00000 | 0 | 0 | 0 |
| 2 | 0·004889 | $3{\cdot}0863 \times 10^{-6}$ | 0·99906 | 0·99326 | 0 | 0 | 0 |
| 3 | $I_3(\alpha)$ | $5{\cdot}8404 \times 10^{-6}$ | 0·99611 | 0·97206 | 0 | 0 | $c_3(\alpha)$ |
| 4 | 0·011603 | $5{\cdot}2920 \times 10^{-5}$ | 0·97275 | 0·80708 | 1·3390 | 0·4992 | 0 |
| 5 | 0·164264 | $e_{5,6}$ | 0·73921 | − 0·81838 | 0·8491 | 0·1516 | 0 |

*Note*: $e_{5\cdot6} = 8{\cdot}3451 \times 10^{-5}$ (mode-1) and $1{\cdot}742 \times 10^{-4}$ (mode-2); and $I_3(\alpha)$ is given in Figure 3·

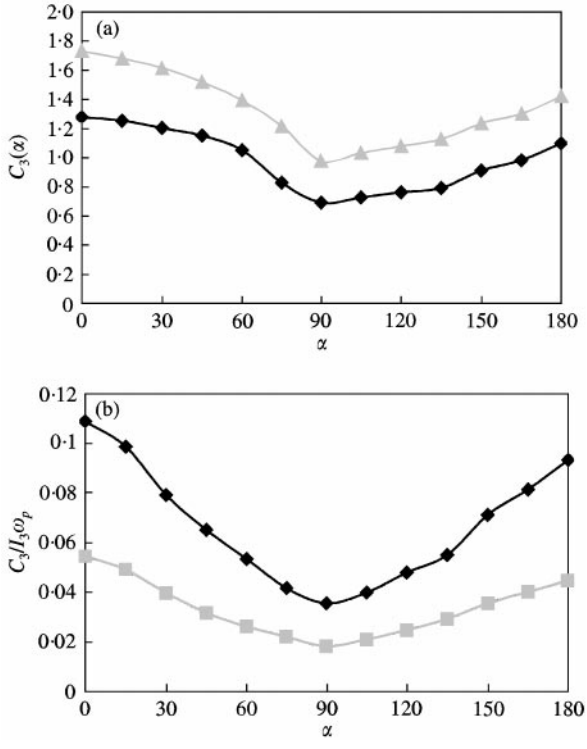


Figure 6. Effect of crank angle position relative to the vertical axis ont he effective single-cylinder damping: (a) absolute damping coefficient $c_3$; —◆—, mode 1; —▲—, mode 2; (b) dimensionless damping parameter $c_3/(I_3\omega_p)$; —◆—, mode 1; —■—, mode 2.

calculation along with the required measurement is performed for different crank positions at each discrete interval of 15°. The results of $c_3$ and the corresponding dimensionless damping term $c_3/(I_3\omega_p)$ depict a distinct U-shape dependency on $\alpha$ ranging from 0 to 180 as shown in Figure 6. This trend indicates the largest damping effect at the $\alpha = 0$ and $\pi$ positions. Since we can infer from equations (4b) and (6b) that the damping from the reciprocating parts is smallest at $\alpha = 0$ and maximum at $\alpha = \pi/2$ rad, while the trend of the damping from the crank–connecting rod interface areas are the opposite, we can conclude that the damping from the crank–connecting rod interface areas must be larger. This is also

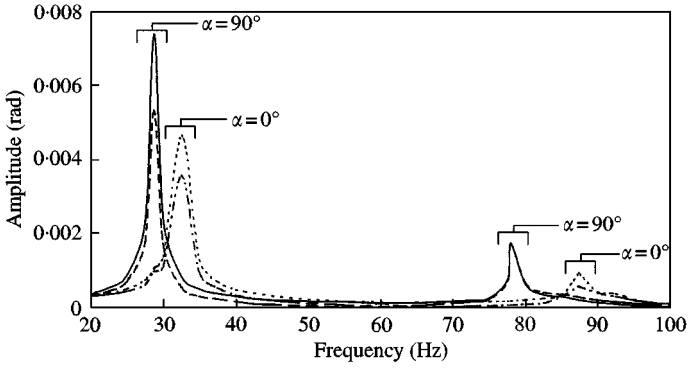


Figure 7. Frequency response spectra of points 1 and 3 for the case of $\alpha = 0$ and $\pi/2$ rad: ——, $\alpha = 90°$, point 1; – – –, $\alpha = 90°$, point 3; - - -, $\alpha = 0°$, point 1; – · · –, $\alpha = 0°$, point 3.

seen in Figure 7 illustrating the frequency response functions of $\varphi_1$ and $\varphi_3$ because the resonance peak for the case of $\alpha = \pi/2$ rad is narrower and higher (which is a symptom of lower damping) than that of the $\alpha = 0$ case. Also, the natural frequency of the former case is slightly lower as previously shown in Figure 3. Detailed analysis of the breakdown of specific damping coefficients from the various energy dissipation causes in the cylinder is beyond the scope of this communication and is left for future research.

To further verify the time-varying damping coefficient results, the complete system is operated in a speed swap mode from about 280–1400 r.p.m. using the motor as the drive to seek out the first two non-zero frequency resonances. Unlike earlier running test to determine $c_8$, the universal joint misalignment angle $\theta$ in this case is set to 0. Hence, the torsional excitation is assumed to come from the reciprocating parts of the cylinder only. Therefore, one can show that the harmonic torque at the cylinder point is classically [1] given by

$$T_3 = (m_s + m_A)(R\Omega)^2 \left[\frac{\lambda}{4}\sin(\Omega t) - \frac{1}{2}\sin(2\Omega t) - \frac{3\lambda}{4}\sin(3\Omega t) - \frac{\lambda^2}{4}\sin(4\Omega t)\right]. \tag{11}$$

Applying equation (8) once more to modes 1 and 2, and using average inertia value for the cylinder shown in Table 1 gives

$$|T_3|\Delta_3 = \omega_p \varphi_1 [\tilde{c}_3 \Delta_3^2 + c_8 \Delta_8^2 + c_{4,5}(\Delta_4 - \Delta_5)^2 + c_{5,6}(\Delta_5 - \Delta_6)^2], \tag{12}$$

which can be used to compute the absolute damping coefficients of the single-cylinder for the $\omega_1$ and $\omega_2$ natural frequencies. This calculation resulted in $c_3 = 0{\cdot}9407$ and 1·3986 Nms/rad for the first and second flexible modes respectively. These running test results are in fact quite close to the time-average damping of 0·9673 Nms/rad (mode 1) and 1·3162 Nms/rad (mode 2) that have been obtained by integrating the time-varying $c_3(\alpha)$ over a full crank cycle and dividing the outcome by $2\pi$ rad.

## 4. CONCLUDING REMARKS

In this communication, we have discussed a relatively straightforward quasi-static experiment to determine the damping coefficients of a single cylinder in terms of the crank angle position. The approach relies on the vibratory energy balance formulation,

and utilizes the measured torsional response of limited points in the set-up. Also, a corresponding motorized experiment can be used to obtain the average damping observed in a running condition, which matches well with the time-average damping data derived from numerically averaging the time-varying damping over one full crank cycle. The resulting damping coefficients can be used to perform linear or time-varying forced response analysis of reciprocating engine systems with one or more cylinders. Our analysis also reveals an interesting result showing the damping effect in the crank-connecting rod interface areas to be more dominant than the net damping level observed in the reciprocating parts. Although the proposed method is demonstrated on a reciprocating single-cylinder engine set-up, its basic procedure is applicable to other damping elements in the powertrain system.

## REFERENCES


1. J. P. Den Hartog 1985 *Mechanical Vibrations*. New York: Dover Publications.
2. B. Z. Li and Q. G. Ying 1988 *Transactions of Chinese Society for Internal Combustion Engines* **6**, 109–120. Torsional vibration characteristics of an engine shaft running at low frequency ratio.
3. K. Tsuda 1967 *Science of Machines* **1**, 279–283. Vibration of internal combustion engine.
4. S. M. Athavale and P. R. Sajanpawar 1999 SAE Paper 1999-01-1769. Analytical studies on influence of crankshaft vibrations on engine noise integrated parametric finite element model: quick assessment tool.
5. T. Morita and H. Okamura 1995 *SAE Paper* 951292. Analysis of crankshaft three-dimensional vibrations in a rotating coordinate system.
6. J. F. Shannon 1935 *Proceedings of the Institution of Mechanical Engineers* **131**, 387–435. Damping influences in torsional oscillation.
7. E. J. Nestorides (editor) (The British Internal Combustion Engine Research Association) 1958. *Handbook on Torsional Vibration*. London: Cambridge University Press.
8. P. Draminsky 1948 *Proceedings of the Institution of Mechanical Engineers* **159**. Crank damping.
9. W. Ker Wilson 1963 *Practical Solution of Torsional Vibration Problems*. New York: John Wiley & Sons Inc.
10. Y. Wang, S. T. Song and X. G. Song 1996 *Journal of Dalian University of Technology* **36**, 590–594. Comment on empirical formulas for calculating marine engine damping coefficient.
11. S. Iwamoto and K. Wakabayashi 1985 *Journal of the Marine Engineering Society* **20**. A study on the damping characteristics of torsional vibration in diesel engines.
12. B. Z. Li and Q. G. Ying 1984 *Torsional Vibration in Internal Combustion Engine Shaft Systems*. Beijing, People's Republic of China: Goufang Publishing House.